Branching ratio and CP asymmetry of $B_s \to K_0^*(1430)\eta^{(\prime)}$ decays in the PQCD approach *

ZHANG Zhi-Qing(张志清)[1)] WANG Shi-Jian(王世建) ZHANG Li-Ying(张丽英)

Department of Physics, Henan University of Technology, Zhengzhou 450001, China

Abstract: In the two-quark model supposition for $K_0^*(1430)$, which can be viewed as either the first excited state (Scenario Ⅰ) or the lowest lying state (Scenario Ⅱ), the branching ratios and the direct CP-violating asymmetries for decays $\bar{B}_s^0 \to K_0^{*0}(1430)\eta^{(\prime)}$ are studied by employing the perturbative QCD factorization approach. We find the following results: (a) The CP averaged branching ratios of $\bar{B}_s^0 \to K_0^{*0}(1430)\eta$ and $\bar{B}_s^0 \to K_0^{*0}(1430)\eta'$ are small and both in the order of 10^{-7}. If one views $K_0^*(1430)$ as the lowest lying state, $\mathcal{B}(\bar{B}_s^0 \to K_0^{*0}(1430)\eta) \approx 3.9\times10^{-7}$ and $\mathcal{B}(\bar{B}_s^0 \to K_0^{*0}(1430)\eta') \approx 7.8\times10^{-7}$. (b) While the direct CP-violating asymmetries of these two decays are not small: if we still take the parameters of $K_0^*(1430)$ in scenario Ⅱ, $\mathcal{A}_{CP}^{\rm dir}(\bar{B}_s^0 \to K_0^{*0}(1430)\eta) \approx 56.2\%$ and $\mathcal{A}_{CP}^{\rm dir}(\bar{B}_s^0 \to K_0^{*0}(1430)\eta') \approx 42.4\%$. (c) The annihilation contributions will play an important role in accounting for future data, because both the branching ratios and the direct CP asymmetries of these two decays are sensitive to the annihilation type contributions.

Key words: PQCD approach, B_s meson decay, scalar meson

PACS: 13.25.Hw, 12.38.Bx, 14.40.Nd **DOI:** 10.1088/1674-1137/37/4/043103

1 Introduction

Together with the many scalar mesons found in experiments, more and more effort has been made to theoretically study the scalar meson spectrum [1–7]. Today, it is still a difficult but interesting topic. Our most important task is to uncover the mysterious structures of the scalar mesons. There are two typical schemes for their classification [1, 2]. Scenario I(SI): the nonet mesons below 1 GeV, including $f_0(600)$, $f_0(980)$, $K_0^*(800)$, and $a_0(980)$, are usually viewed as the lowest lying $q\bar{q}$ states, while the nonet ones near 1.5 GeV, including $f_0(1370)$, $f_0(1500)/f_0(1700)$, $K_0^*(1430)$, and $a_0(1450)$, are suggested as the first excited states. In Scenario Ⅱ (SⅡ), the nonet mesons near 1.5 GeV are treated as $q\bar{q}$ ground states, while the nonet mesons below 1 GeV are exotic states beyond the quark model, such as the four-quark bound states.

As for the structure of the pseudo-scalar meson $\eta^{(\prime)}$, the uncertainty is less than that of the scalar meson, it is generally considered as a linear combination of light quark pairs $u\bar{u}$, $d\bar{d}$ and $s\bar{s}$. Furthermore, many studies [8, 9] show that the gluon component in the meson $\eta^{(\prime)}$ is small and can be neglected. In the quark-flavor mixing scheme, the physical states η and η' are related to the flavor states $\eta_q=(u\bar{u}+d\bar{d})/\sqrt{2}$ and $\eta_s=s\bar{s}$ through a single mixing angle ϕ,

$$\begin{pmatrix}\eta\\ \eta'\end{pmatrix} = \begin{pmatrix}\cos\phi & -\sin\phi\\ \sin\phi & \cos\phi\end{pmatrix}\begin{pmatrix}\eta_q\\ \eta_s\end{pmatrix} = \begin{pmatrix}F_1(\phi)(u\bar{u}+d\bar{d})+F_2(\phi)s\bar{s}\\ F_1'(\phi)(u\bar{u}+d\bar{d})+F_2'(\phi)s\bar{s}\end{pmatrix}, \quad (1)$$

with

$$F_1(\phi) = \frac{\cos\phi}{\sqrt{2}}, \quad F_2(\phi)=-\sin\phi,$$
$$F_1'(\phi) = \frac{\sin\phi}{\sqrt{2}}, \quad F_2'(\phi)=\cos\phi, \quad (2)$$

where $\phi=39.3^\circ\pm1.0^\circ$.

In order to uncover the inner structures of the scalar mesons, many factorization approaches are used to research the B meson decay modes with a final state scalar meson, such as the generalized factorization approach [10], QCD factorization (QCDF) approach [11–13], and perturbative QCD (PQCD) approach [14–16]. The decays $B \to K_0^{*0}(1430)\eta^{(\prime)}$ have been studied using QCDF by Cheng and Chua [17]. They conclude that Scenario Ⅱ is more preferable than Scenario Ⅰ, because the predictions in Scenario Ⅱ account for the present experimental

Received 28 May 2012, Revised 11 July 2012

∗ Supported by National Natural Science Foundation of China (11147004) and Foundation of Henan University of Technology (2009BS038)

1) E-mail: zhangzhiqing@haut.edu.cn

results better. For example, the branching ratios of decays $\bar{B}^0\to\bar{K}_0^{*0}(1430)\eta$ and $\bar{B}^0\to\bar{K}_0^{*0}(1430)\eta'$ in Scenario II predicted by the QCDF approach are 12.6×10^{-6} and 8.7×10^{-6} respectively, which are consistent with the experimental values $(9.6\pm1.9)\times10^{-6}$ and $(6.3\pm1.6)\times10^{-6}$. While the predictions in Scenario I are 0.4×10^{-6} and 26.6×10^{-6} respectively, neither of them is consistent with the data. Furthermore, the authors argue that the rate of $B\to K_0^{*0}(1430)\eta$ is slightly larger than that of $K_0^{*0}(1430)\eta'$ owing to the fact that the η-η' mixing angle ϕ between η_q and η_s is less than 45°. We want to investigate if the same condition also occurs in the decays $\bar{B}_s\to K_0^{*0}(1430)\eta^{(\prime)}$.

Certainly, $K_0^*(1430)$ can be treated as a $q\bar{q}$ state in both Scenario I and Scenario II, it is easy to make a quantitative prediction in the two-quark model supposition, so we can use the PQCD approach to calculate the branching ratios and the CP-violating asymmetries for decays $\bar{B}_s^0\to K_0^{*0}(1430)\eta^{(\prime)}$ in the two scenarios.

In the following, $K_0^*(1430)$ is denoted as K_0^* in some places for convenience. The layout of this paper is as follows. In Section 2, the decay constants and light-cone distribution amplitudes of the relevant mesons are introduced. In Section 3, we then analyze these decay channels using the PQCD approach. The numerical results and the discussion are given in Section 4. The conclusions are presented in the final part.

2 The decay constants and distribution amplitudes

In general, the B_s meson is treated as a heavy-light system, and its Lorentz structure can be written as [18, 19]

$$\Phi_{B_s}=\frac{1}{\sqrt{2N_c}}(\not{P}_{B_s}+M_{B_s})\gamma_5\phi_{B_s}(k_1). \tag{3}$$

For the distribution amplitude $\phi_{B_s}(x,b)$ in Eq. (3), we adopt the following model:

$$\phi_{B_s}(x,b)=N_{B_s}x^2(1-x)^2\exp\left[-\frac{M_{B_s}^2x^2}{2\omega_b^2}-\frac{(\omega_b b)^2}{2}\right], \tag{4}$$

where ω_{b_s} is a free parameter, we take $\omega_{b_s}=0.5\pm0.05$ GeV in numerical calculations, and $N_{B_s}=63.67$ is the normalization factor for $\omega_b=0.5$. Certainly, the other Lorentz structure $\bar{\phi}_{B_s}$ should be considered, which is given as

$$\bar{\phi}_{B_s}=\frac{f_{B_s}(2x-\Lambda_0)}{\sqrt{6}\Lambda_0^2}\theta(\Lambda_0-x)J_0\left[m_{B_s}b\sqrt{x(\Lambda_0-x)}\right], \tag{5}$$

where $\Lambda_0=2\bar{\Lambda}/m_{B_s}$, and $\bar{\Lambda}$ is a free parameter and in the order of m_{B_s}–m_b. It is easy to see that ϕ_{B_s} is numerically small [20] and so it can be neglected.

In the two-quark picture, the vector decay constant $f_{K_0^*}$ and the scalar decay constant $\bar{f}_{K_0^*}$ for the scalar meson K_0^* can be defined as

$$\langle K_0^*(p)|\bar{q}_2\gamma_\mu q_1|0\rangle = f_{K_0^*}p_\mu, \tag{6}$$

$$\langle K_0^*(p)|\bar{q}_2 q_1|0\rangle = m_{K_0^*}\bar{f}_{K_0^*}, \tag{7}$$

where $m_{K_0^*}(p)$ is the mass (momentum) of the scalar meson K_0^*. The relationship between $f_{K_0^*}$ and $\bar{f}_{K_0^*}$ is

$$\frac{m_{K_0^*}}{m_2(\mu)-m_1(\mu)}f_{K_0^*}=\bar{f}_{K_0^*}, \tag{8}$$

where $m_{1,2}$ are the running current quark masses. For the scalar meson $K_0^*(1430)$, $f_{K_0^*}$ will get a very small value after the $SU(3)$ symmetry breaking is considered. The light-cone distribution amplitudes for the scalar meson $K_0^*(1430)$ can be written as

$$\begin{aligned}&\langle K_0^*(p)|\bar{q}_1(z)_l q_2(0)_j|0\rangle\\ &= \frac{1}{\sqrt{2N_c}}\int_0^1 dx e^{ixp\cdot z}\Big\{\not{p}\Phi_{K_0^*}(x)+m_{K_0^*}\Phi_{K_0^*}^S(x)\\ &\quad +m_{K_0^*}(\not{n}_+\not{n}_- -1)\Phi_{K_0^*}^T(x)\Big\}_{jl}.\end{aligned} \tag{9}$$

Here the number of colors $N_c=3$, n_+ and n_- are lightlike vectors: $n_+=(1,0,0_T)$, $n_-=(0,1,0_T)$, and n_+ is parallel with the moving direction of the scalar meson. The normalization can be related to the decay constants:

$$\int_0^1 dx\Phi_{K_0^*}(x) = \int_0^1 dx\Phi_{K_0^*}^T(x)=0, \tag{10}$$

$$\int_0^1 dx\Phi_{K_0^*}^S(x) = \frac{\bar{f}_{K_0^*}}{2\sqrt{2N_c}}. \tag{11}$$

The twist-2 light-cone distribution amplitude $\Phi_{K_0^*}$ can be expanded in the Gegenbauer polynomials:

$$\begin{aligned}\Phi_{K_0^*}(x,\mu) &= \frac{\bar{f}_{K_0^*}(\mu)}{2\sqrt{2N_c}}6x(1-x)\Big[B_0(\mu)\\ &\quad +\sum_{m=1}^{\infty}B_m(\mu)C_m^{3/2}(2x-1)\Big],\end{aligned} \tag{12}$$

where the decay constant $\bar{f}_{K_0^*}=-300\pm30(445\pm50)$ MeV and the Gegenbauer moments $B_1=0.58\pm0.07(-0.57\pm0.13)$, $B_3=-1.2\pm0.08(-0.42\pm0.22)$ [12] in S I (S II). They are taken by fixing the scale at 1 GeV.

The twist-3 distribution amplitudes are $\Phi_{K_0^*}^S$ and $\Phi_{K_0^*}^T$, we adopt the asymptotic form:

$$\Phi_{K_0^*}^S=\frac{1}{2\sqrt{2N_c}}\bar{f}_{K_0^*}, \quad \Phi_{K_0^*}^T=\frac{1}{2\sqrt{2N_c}}\bar{f}_{K_0^*}(1-2x). \tag{13}$$

As for the distribution amplitudes of the meson $\eta^{(\prime)}$, we take the same functions and parameters as those in Ref. [21].

3 The perturbative QCD calculation

Under the two-quark model for the scalar meson $\mathrm{K}_0^*(1430)$ supposition, the amplitudes for the decays $\bar{\mathrm{B}}_\mathrm{s}^0\to\mathrm{K}_0^*\eta^{(\prime)}$ can be conceptually written as the convolution,

$$\begin{aligned}\mathcal{A}(\bar{\mathrm{B}}_\mathrm{s}^0\to\mathrm{K}_0^*\eta^{(\prime)})\sim&\int\mathrm{d}x_1\mathrm{d}x_2\mathrm{d}x_3b_1\mathrm{d}b_1b_2\mathrm{d}b_2b_3\mathrm{d}b_3\\&\times\mathrm{Tr}\left[C(t)\Phi_{\mathrm{B_s}}(x_1,b_1)\cdot\Phi_{\mathrm{K}_0^*}(x_2,b_2)\Phi_{\eta^{(\prime)}}(x_3,b_3)\right.\\&\left.\times H(x_i,b_i,t)S_\mathrm{t}(x_i)\mathrm{e}^{-S(t)}\right],\end{aligned}\tag{14}$$

where $b_i(i=1,2,3)$ is the conjugate space coordinate of $k_{i\mathrm{T}}$, x_i is the momenta fraction of the antiquark in each meson, and t is the largest energy scale in function $H(x_i,b_i,t)$. Here Tr denotes the trace over the Dirac and the color indices, $C(t)$ is the Wilson coefficient evaluated at scale t, which includes the hard dynamics from m_W which scale down to $t\sim\mathcal{O}(\sqrt{\Lambda M_{\mathrm{B_s}}})$. The function $H(x_i,b_i,t)$ describes the six-quark hard scattering kernel, which consists of the effective four quark operators and a hard gluon to connect the spectator quark in the decay. The hard part H can be perturbatively calculated. $\Phi_{\mathrm{B_s}(\mathrm{K}_0^*,\eta^{(\prime)})}$ is the wave function of the meson $\mathrm{B_s}(\mathrm{K}_0^*,\eta^{(\prime)})$. In order to smear the end-point singularity on x_i, the jet function $S_t(x)$ [22], which comes from the resummation of the double logarithms $\ln^2x_i$, is used. The last term $\mathrm{e}^{-S(t)}$ is the Sudakov form factor which suppresses the soft dynamics effectively [23]. Here we use the light-cone coordinate to describe the meson's momenta. There are the same conventions with Refs. [24, 25] in our calculations.

In the standard model, the related weak effective Hamiltonian H_eff mediating the $\mathrm{b}\to\mathrm{d}$ type transitions can be written as [26]

$$\begin{aligned}\mathcal{H}_\mathrm{eff}=&\frac{G_\mathrm{F}}{\sqrt{2}}\left[\sum_{\mathrm{p=u,c}}V_\mathrm{pb}V_\mathrm{pd}^*(C_1(\mu)O_1^\mathrm{p}(\mu)\right.\\&\left.+C_2(\mu)O_2^\mathrm{p}(\mu))-V_\mathrm{tb}V_\mathrm{td}^*\sum_{i=3}^{10}C_i(\mu)O_i(\mu)\right].\end{aligned}\tag{15}$$

Here the function $Q_i(i=1,\cdots,10)$ is the local four-quark operator and C_i is the corresponding Wilson coefficient. $V_\mathrm{p(t)b}$, $V_\mathrm{p(t)d}$ are the CKM matrix elements. The standard four-quark operators are defined as:

$$\begin{aligned}O_1^\mathrm{u}&=\bar{d}_\alpha\gamma^\mu Lu_\beta\cdot\bar{u}_\beta\gamma_\mu Lb_\alpha,\\O_2^\mathrm{u}&=\bar{d}_\alpha\gamma^\mu Lu_\alpha\cdot\bar{u}_\beta\gamma_\mu Lb_\beta,\\O_3&=\bar{d}_\alpha\gamma^\mu Lb_\alpha\cdot\sum_{\mathrm{q}'}\bar{q}'_\beta\gamma_\mu Lq'_\beta,\\O_4&=\bar{d}_\alpha\gamma^\mu Lb_\beta\cdot\sum_{\mathrm{q}'}\bar{q}'_\beta\gamma_\mu Lq'_\alpha,\\O_5&=\bar{d}_\alpha\gamma^\mu Lb_\alpha\cdot\sum_{\mathrm{q}'}\bar{q}'_\beta\gamma_\mu Rq'_\beta,\\O_6&=\bar{d}_\alpha\gamma^\mu Lb_\beta\cdot\sum_{\mathrm{q}'}\bar{q}'_\beta\gamma_\mu Rq'_\alpha,\\O_7&=\frac{3}{2}\bar{d}_\alpha\gamma^\mu Lb_\alpha\cdot\sum_{\mathrm{q}'}e_{\mathrm{q}'}\bar{q}'_\beta\gamma_\mu Rq'_\beta,\\O_8&=\frac{3}{2}\bar{d}_\alpha\gamma^\mu Lb_\beta\cdot\sum_{\mathrm{q}'}e_{\mathrm{q}'}\bar{q}'_\beta\gamma_\mu Rq'_\alpha,\\O_9&=\frac{3}{2}\bar{d}_\alpha\gamma^\mu Lb_\alpha\cdot\sum_{\mathrm{q}'}e_{\mathrm{q}'}\bar{q}'_\beta\gamma_\mu Lq'_\beta,\\O_{10}&=\frac{3}{2}\bar{d}_\alpha\gamma^\mu Lb_\beta\cdot\sum_{\mathrm{q}'}e_{\mathrm{q}'}\bar{q}'_\beta\gamma_\mu Lq'_\alpha,\end{aligned}\tag{16}$$

where α and β are the $SU(3)$ color indices; L and R are the left- and right-handed projection operators with $L=(1-\gamma_5)$, $R=(1+\gamma_5)$. The sum over q′ runs over the quark fields that are active at the scale $\mu=O(m_\mathrm{b})$, i.e., (q′ϵ{u,d,s,c,b}). It is well known that there are eight leading order Feynman diagrams for the channel $\bar{\mathrm{B}}_\mathrm{s}^0\to\mathrm{K}_0^{*0}(1430)\eta^{(\prime)}$. Certainly, there also exist the contributions from the diagrams by exchanging the position of K_0^* and $\eta^{(\prime)}$ in each Feynman diagram for our considered two decays. Here we don't give these Feynman diagrams. Combining the contributions from different diagrams, the total decay amplitude for $\bar{\mathrm{B}}_\mathrm{s}^0\to\mathrm{K}_0^{*0}(1430)\eta$ can be written as

$$\begin{aligned}\sqrt{2}\mathcal{M}(\mathrm{K}_0^{*0}\eta)=&\,\xi_\mathrm{u}\left[M_{\mathrm{eK}_0^*}C_2F_1(\phi)+f_\eta^\mathrm{q}F_{\mathrm{eK}_0^*}a_2\right]-\xi_\mathrm{t}\left[f_\eta^\mathrm{q}F_{\mathrm{eK}_0^*}\left(\frac{7C_3}{3}+\frac{5C_4}{3}-2a_5-\frac{a_7}{2}+\frac{C_9}{3}-\frac{C_{10}}{3}\right)\right.\\&+f_\eta^\mathrm{s}F_{\mathrm{eK}_0^*}\left(a_3-a_5+\frac{a_7}{2}-\frac{a_9}{2}\right)+\left(f_\eta^\mathrm{q}F_{\mathrm{eK}_0^*}^{\mathrm{P2}}+f_{\mathrm{K}_0^*}F_{\mathrm{e}\eta}^{\mathrm{P2}}F_2(\phi)\right)\left(a_6-\frac{a_8}{2}\right)+M_{\mathrm{e}\eta}\left(C_3-\frac{C_9}{2}\right)F_2(\phi)\\&+(M_{\mathrm{aK}_0^*}F_1(\phi)+M_{\mathrm{a}\eta}F_2(\phi))\left(C_3-\frac{C_9}{2}\right)+(M_{\mathrm{aK}_0^*}^{\mathrm{P1}}F_1(\phi)+M_{\mathrm{a}\eta}^{\mathrm{P1}}F_2(\phi))\left(C_5-\frac{C_7}{2}\right)+M_{\mathrm{eK}_0^*}^{\mathrm{P2}}\left(C_6-\frac{C_8}{2}\right)F_2(\phi)\\&\left.+f_{\mathrm{B_s}}(F_{\mathrm{aK}_0^*}F_1(\phi)+F_{\mathrm{a}\eta}F_2(\phi))\left(a_4-\frac{a_{10}}{2}\right)+f_{\mathrm{B_s}}(F_{\mathrm{aK}_0^*}^{\mathrm{P2}}F_1(\phi)+F_{\mathrm{a}\eta}^{\mathrm{P2}}F_2(\phi))\left(a_6-\frac{a_8}{2}\right)\right.\end{aligned}$$

$$+M_{\mathrm{eK}_0^*}\left(C_3+2C_4-\frac{C_9}{2}+\frac{1}{2}C_{10}\right)F_1(\phi)+M_{\mathrm{eK}_0^*}\left(C_4-\frac{1}{2}C_{10}\right)F_2(\phi)$$
$$+\left(M^{\mathrm{P1}}_{\mathrm{eK}_0^*}F_1(\phi)+M^{\mathrm{P1}}_{\mathrm{e}\eta}F_2(\phi)\right)\left(C_5-\frac{1}{2}C_7\right)+M^{\mathrm{P2}}_{\mathrm{eK}_0^*}\left(2C_6+\frac{1}{2}C_8\right)F_1(\phi)\Big], \quad (17)$$

where $\xi_{\mathrm{u}}=V^*_{\mathrm{ub}}V_{\mathrm{ud}}$, $\xi_{\mathrm{t}}=V^*_{\mathrm{tb}}V_{\mathrm{td}}$, while $F_{\mathrm{e(a)K}_0^*}$ and $M_{\mathrm{e(a)K}_0^*}$ are the $\eta^{(\prime)}$ meson emission (annihilation) factorizable contributions and nonfactorizable contributions from penguin operators, respectively. The upper label T denotes the contributions from tree operators. Similarly, $F_{\mathrm{e(a)}\eta^{(\prime)}}$ and $M_{\mathrm{e(a)}\eta^{(\prime)}}$ are the $\mathrm{K}_0^*(1430)$ meson emission (annihilation) factorizable contributions and nonfactorizable contributions from penguin operators, respectively. $F_1(\phi)$ and $F_2(\phi)$ are the mixing factors as given in Eq. (2). f^{q}_η and f^{s}_η are the decay constants of the flavor states η_{q} and η_{s}, respectively. The complete decay amplitude for $\bar{\mathrm{B}}^0_{\mathrm{s}}\to\mathrm{K}_0^{*0}(1430)\eta'$ can be obtained from the upper equation by the following replacements:

$$f^{\mathrm{q}}_\eta\to f^{\mathrm{q}}_{\eta'}, f^{\mathrm{s}}_\eta\to f^{\mathrm{s}}_{\eta'}, F_1(\phi)\to F_1'(\phi), F_2(\phi)\to F_2'(\phi). \quad (18)$$

The combinations of the Wilson coefficients are defined as usual [21]:

$$\begin{aligned} a_1(\mu) &= C_2(\mu)+\frac{C_1(\mu)}{3}, \quad a_2(\mu)=C_1(\mu)+\frac{C_2(\mu)}{3},\\ a_i(\mu) &= C_i(\mu)+\frac{C_{i+1}(\mu)}{3}, \quad i=3,5,7,9,\\ a_i(\mu) &= C_i(\mu)+\frac{C_{i-1}(\mu)}{3}, \quad i=4,6,8,10. \end{aligned} \quad (19)$$

4 Numerical results and discussions

We use the following input parameters in the numerical calculations:

$$f_{\mathrm{B_s}} = 230\ \mathrm{MeV},\ M_{\mathrm{B_s}}=5.37\ \mathrm{GeV}, \quad (20)$$
$$\alpha = 100^\circ\pm20^\circ,\ \tau_{\mathrm{B_s}}=1.470\times10^{-12}\ \mathrm{s}, \quad (21)$$
$$|V_{\mathrm{ub}}| = 3.89\times10^{-3},\ V_{\mathrm{ud}}=0.974, \quad (22)$$
$$|V_{\mathrm{td}}| = 8.4\times10^{-3},\ V_{\mathrm{tb}}=1.0. \quad (23)$$

In the $\mathrm{B_s}$-rest frame, the decay rates of $\bar{\mathrm{B}}^0_{\mathrm{s}}\to\mathrm{K}_0^*(1430)\eta^{(\prime)}$ can be written as

$$\Gamma=\frac{G_{\mathrm{F}}^2}{32\pi m_{\mathrm{B_s}}}|\mathcal{M}|^2(1-r^2_{\mathrm{K}_0^*}), \quad (24)$$

where the mass ratio $r_{\mathrm{K}_0^*}=m_{\mathrm{K}_0^*}/M_{\mathrm{B}^0_{\mathrm{s}}}$ and $\mathcal{M}$ is the total decay amplitude of each considered decay, which can be found in Sec. 3. The $\mathcal{M}$ can be rewritten as

$$\mathcal{M}=V_{\mathrm{ub}}V^*_{\mathrm{ud}}T-V_{\mathrm{tb}}V^*_{\mathrm{td}}P=V_{\mathrm{ub}}V^*_{\mathrm{ud}}\left[1+z\mathrm{e}^{\mathrm{i}(\alpha+\delta)}\right], \quad (25)$$

where α is the Cabibbo-Kobayashi-Maskawa weak phase angle, and δ is the relative strong phase between the tree and the penguin amplitudes, which are denoted as "T" and "P", respectively. The term z describes the ratio of penguin to tree contributions and is defined as

$$z=\left|\frac{V_{\mathrm{tb}}V^*_{\mathrm{td}}}{V_{\mathrm{ub}}V^*_{\mathrm{ud}}}\right|\left|\frac{P}{T}\right|. \quad (26)$$

From Eq. (25), it is easy to write decay amplitude $\overline{\mathcal{M}}$ for the corresponding conjugated decay mode. So the CP-averaged branching ratio for each considered decay is defined as

$$\begin{aligned}\mathcal{B} &= (|\mathcal{M}|^2+|\overline{\mathcal{M}}|^2)/2\\ &= |V_{\mathrm{ub}}V^*_{\mathrm{ud}}T|^2[1+2z\cos\alpha\cos\delta+z^2].\end{aligned} \quad (27)$$

The direct CP-violating asymmetry can be defined as

$$\mathcal{A}^{\mathrm{dir}}_{CP}=\frac{|\overline{\mathcal{M}}|^2-|\mathcal{M}|^2}{|\mathcal{M}|^2+|\overline{\mathcal{M}}|^2}=\frac{2z\sin\alpha\sin\delta}{1+2z\cos\alpha\cos\delta+z^2}. \quad (28)$$

Using the input parameters and the wave functions as specified in this and previous sections, it is easy to get the values of the factorizable and nonfactorizable amplitudes from the emission and annihilation topology diagrams of the considered decays in both scenarios, which are listed in Table 1. For the decay $\bar{\mathrm{B}}^0_{\mathrm{s}}\to\mathrm{K}_0^{*0}(1430)\eta'$, the tree contribution from the emission factorizable diagrams is color suppressed, so the corresponding amplitude is not very large. The amplitudes $F_{\mathrm{eK}_0^*}$ for each decay are very small from the $\mathrm{u\bar{u}}$ and $\mathrm{d\bar{d}}$ quark components in the meson $\eta^{(\prime)}$, while they are large from the $\mathrm{s\bar{s}}$ component, which have contrary signs between decay modes $\mathrm{K}_0^{*0}(1430)\eta$ and $\mathrm{K}_0^{*0}(1430)\eta'$: the amplitudes $F^{\mathrm{SP}}_{\mathrm{eK}_0^*}$ and $F^{\mathrm{VA}}_{\mathrm{eK}_0^*}$ weaken each other for the former, and reinforce each other for the latter. Here $F^{\mathrm{SP}}_{\mathrm{eK}_0^*}$ and $F^{\mathrm{VA}}_{\mathrm{eK}_0^*}$ represent the amplitudes corresponding to the $(S-P)(S+P)$ currents and $(V-A)(V\pm A)$ currents, respectively. So the amplitude $F_{\mathrm{eK}_0^*}$ is small for the decay $\bar{\mathrm{B}}^0_{\mathrm{s}}\to\mathrm{K}_0^{*0}(1430)\eta$, while it is large for the decay $\bar{\mathrm{B}}^0_{\mathrm{s}}\to\mathrm{K}_0^{*0}(1430)\eta'$, especially in Scenario Ⅱ. The ratio of penguin to tree amplitudes P/T for the decay $\bar{\mathrm{B}}^0_{\mathrm{s}}\to\mathrm{K}_0^{*0}(1430)\eta$ is about 38.5% for Scenario Ⅰ, 57.0% for Scenario Ⅱ. It is about half of the ratio P/T for the decay $\bar{\mathrm{B}}^0_{\mathrm{s}}\to\mathrm{K}_0^{*0}(1430)\eta'$, which is about 77.8% for Scenario Ⅰ, 125% for Scenario Ⅱ. For the decay mode $\mathrm{K}_0^{*0}(1430)\eta'$ in Scenario Ⅱ, its penguin contributions are larger than its tree contributions. It is noticed that the amplitude $F_{\mathrm{e}\eta^{(\prime)}}$ is proportional to the vector decay constant $f_{\mathrm{K}_0^*}$ which is very small, so $F_{\mathrm{e}\eta^{(\prime)}}$ is much smaller compared with $F_{\mathrm{eK}_0^*}$. From Table 1, we also find that the contributions from the factorizable annihilation diagrams are large owing to the chiral enhancements, usually receiving a large imaginary part.

Table 1. Decay amplitudes for decays $\bar{B}_s^0 \to K_0^{*0}(1430)\eta$, $K_0^{*0}(1430)\eta'$ ($\times 10^{-2}$GeV^3).

decay mode	$F^{T}_{eK_0^*}$	$F_{eK_0^*}$	$M^{T}_{eK_0^*}$	$M_{eK_0^*}$	$M_{aK_0^*}$	$F_{aK_0^*}$
$\bar{B}_s^0 \to K_0^{*0}\eta$ (S I)	−11.10	1.80	−5.41+3.76i	−0.25−0.36i	−0.02−0.06i	2.69+6.69i
$\bar{B}_s^0 \to K_0^{*0}\eta$ (S II)	13.66	−2.03	0.22+3.24i	−0.02−0.11i	−0.14−0.09i	0.53−8.97i
$\bar{B}_s^0 \to K_0^{*0}\eta'$ (S I)	−9.09	8.42	−4.43+3.08i	−0.60−2.98i	0.08−0.04i	2.20+5.47i
$\bar{B}_s^0 \to K_0^{*0}\eta'$ (S II)	11.18	−12.30	0.18+2.65i	−0.20−1.34i	−0.12−0.07i	0.43−7.35i
decay mode	$F_{e\eta^{(\prime)}}$	$M_{e\eta^{(\prime)}}$	$M_{a\eta^{(\prime)}}$	$F_{a\eta^{(\prime)}}$		
$\bar{B}_s^0 \to K_0^{*0}\eta$ (S I)	0.09	0.52−1.31i	0.50−0.74i	0.83−2.24i	—	—
$\bar{B}_s^0 \to K_0^{*0}\eta$ (S II)	−0.13	−0.94−0.58i	−0.70+0.04i	−1.37+3.16i	—	—
$\bar{B}_s^0 \to K_0^{*0}\eta'$ (S I)	−0.11	−0.63+1.60i	−0.61+0.90i	−1.08+2.74i	—	—
$\bar{B}_s^0 \to K_0^{*0}\eta'$ (S II)	0.16	1.15+0.71i	0.86−0.05i	1.67−3.87i	—	—

The importance of the factorizable annihilation contributions will be further discussed in the latter.

Using the input parameters and the wave functions as specified in this section and Sec. 2, we can calculate the branching ratios of the considered decay modes in 10^{-7} order

$$\mathcal{B}(\bar{B}_s^0 \to K_0^{*0}\eta) = 3.85^{+1.48+0.81+0.41+0.91}_{-1.01-0.77-0.37-0.96}\,\mathrm{S\,I}\,,$$

$$\mathcal{B}(\bar{B}_s^0 \to K_0^{*0}\eta') = 5.17^{+1.60+1.09+0.60+0.76}_{-1.01-0.98-0.56-0.80}\,\mathrm{S\,I}\,,$$

$$\mathcal{B}(\bar{B}_s^0 \to K_0^{*0}\eta) = 3.87^{+1.22+0.89+2.22+0.84}_{-0.83-0.80-1.73-0.90}\,\mathrm{S\,II}\,,$$

$$\mathcal{B}(\bar{B}_s^0 \to K_0^{*0}\eta') = 7.75^{+2.09+1.80+3.14+1.21}_{-1.30-1.61-2.65-1.28}\,\mathrm{S\,II}\,,$$

where the uncertainties are mainly from the B_s meson shape parameter ω_{b_s}, the decay constant $\bar{f}_{K_0^*}$, the Gegenbauer moments B_1 and B_3 of the scalar meson K_0^*, and the CKM angle $\alpha = (100 \pm 20)^\circ$. The branching ratios in scenario II are more sensitive to the Gegenbauer moments of K_0^* than those in Scenario I. For the decay $\bar{B}_s^0 \to K_0^{*0}(1430)\eta$, its branching ratios in these two scenarios are almost equal to each other. From the results, one can find that the branching ratio of the decay channel $\bar{B}_s^0 \to K_0^{*0}(1430)\eta'$ is larger than that of $\bar{B}_s^0 \to K_0^{*0}(1430)\eta$. It is possible that the mechanism which induces the so-called $K\eta'$-puzzle in the decays $B \to K\eta^{(\prime)}$ [21] also occurs in the considered decays, but is merely not very sharp. Similarly, it is also found in the decays $B \to K_2^*(1430)\eta^{(\prime)}$, $B_s \to K\eta^{(\prime)}$, while the situation is contrary to the decays $B \to K_0^*(1430)\eta^{(\prime)}$ and $B \to K^*\eta^{(\prime)}$ (shown in Table 2): the branching ratios of decays involving the η' meson are smaller than those of the decays involving the η meson. In a word, these characters are induced by the constructive or destructive interference between different types of penguin contributions [17] for these decays. According to the QCDF approach [17], $K_0^*(1430)$ is viewed as the lowest-lying P-wave $q\bar{q}$ meson (Scenario II), which has been confirmed by the lattice calculations [30]. Certainly, it needs to be verified by future experiments. By using the $SU(3)$ symmetry, one can relate the decays $B \to \pi^0\eta^{(\prime)}$ with our considered ones, So $\mathcal{B}(B \to \pi^0\eta^{(\prime)})$ are also listed in Table 2. For the branching ratio of decay $B \to \pi^0\eta$, only the upper limit can be obtained. The theoretical values for $\mathcal{B}(B \to \pi^0\eta)$ predicted by the QCDF and PQCD approach are $(0.28^{+0.48}_{-0.28})\times 10^{-6}$ [31] and $(0.23 \pm 0.08)\times 10^{-6}$ [32], respectively. The dependence of the branching ratios for the decays $\bar{B}_s^0 \to K_0^{*0}(1430)\eta$ and $\bar{B}_s^0 \to K_0^{*0}(1430)\eta'$ on the Cabibbo-Kobayashi-Maskawa angle α are displayed in Fig. 1.

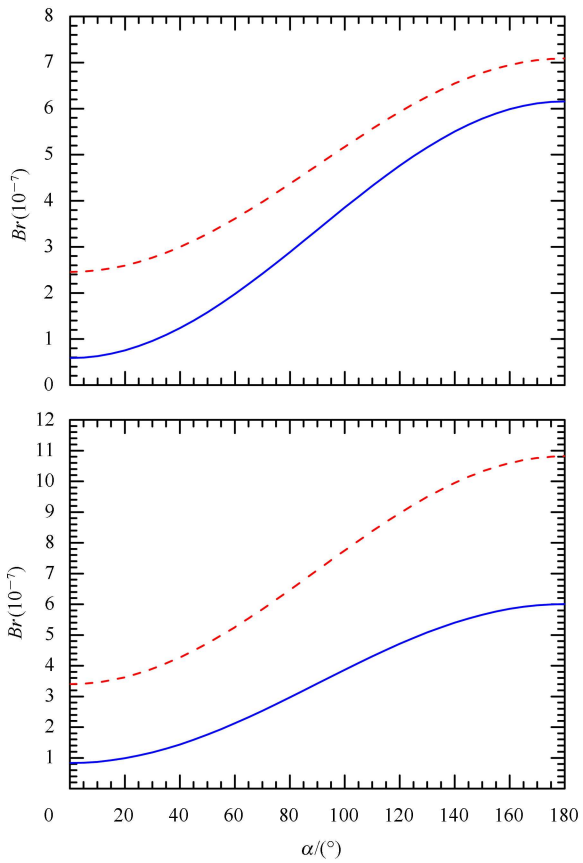

Fig. 1. The dependence of the branching ratios for $\bar{B}_s^0 \to K_0^{*0}(1430)\eta$ (solid curve) and $\bar{B}_s^0 \to K_0^{*0}(1430)\eta'$ (dashed curve) on the Cabibbo-Kobayashi-Maskawa angle α. The up (down) panel is plotted in Scenario I (II).

Table 2. Branching ratios of decays $B \to K\eta^{(\prime)}$, $K_2^*(1430)\eta^{(\prime)}$, $B \to K^*\eta^{(\prime)}$, $K_0^*(1430)\eta^{(\prime)}$ and $\bar{B}_s^0 \to K\eta^{(\prime)}$. The data in the first column are for the decays involving the η meson.

decay mode	Exp. [27]($\times 10^{-6}$)	Exp. [27]($\times 10^{-6}$)
$B^- \to K^-\eta^{(\prime)}$	2.36 ± 0.27	71.1 ± 2.6
$\bar{B}^0 \to \bar{K}^0\eta^{(\prime)}$	$1.12^{+0.30}_{-0.28}$	66.1 ± 3.1
$B^- \to K_2^{*-}\eta^{(\prime)}$	9.1 ± 3.0	$28.0^{+5.3}_{-5.0}$
$\bar{B}^0 \to \bar{K}_2^{*0}\eta^{(\prime)}$	9.6 ± 2.1	$13.7^{+3.2}_{-2.2}$
$B^- \to K^{*-}\eta^{(\prime)}$	19.3 ± 1.6	$5.0^{+1.8}_{-1.6}$
$\bar{B}^0 \to \bar{K}^{*0}\eta^{(\prime)}$	15.9 ± 1.0	3.1 ± 0.9
$B^- \to K_0^{*-}\eta^{(\prime)}$	15.8 ± 3.1	5.2 ± 2.1
$\bar{B}^0 \to \bar{K}_0^{*0}\eta^{(\prime)}$	9.6 ± 1.9	6.3 ± 1.6
	PQCD[28]($\times 10^{-7}$)	PQCD[28]($\times 10^{-7}$)
$\bar{B}_s^0 \to K^0\eta^{(\prime)}$	$1.1^{+0.8}_{-0.4}$	$7.2^{+3.6}_{-2.4}$
	Exp. [29]($\times 10^{-6}$)	Exp. [29]($\times 10^{-6}$)
$\bar{B}^0 \to \pi^0\eta^{(\prime)}$	<1.5	$0.9\pm0.4\pm0.1$

Using the calculated ratio z and strong phase δ, it is easy to find the numerical values of $\mathcal{A}_{CP}^{\rm dir}$ (in units of 10^{-2}) as follows by using the input parameters listed previously for the considered decays in two scenarios:

$$\mathcal{A}_{CP}^{\rm dir}(\bar{B}_s^0 \to K_0^{*0}\eta) = 42.1^{+6.9+0.0+2.8+14.2}_{-5.9-0.0-3.3-12.1}\,{\rm S\,I}\,,$$

$$\mathcal{A}_{CP}^{\rm dir}(\bar{B}_s^0 \to K_0^{*0}\eta') = 70.9^{+2.8+0.0+2.8+13.0}_{-6.0-0.0-2.9-16.5}\,{\rm S\,I}\,,$$

$$\mathcal{A}_{CP}^{\rm dir}(\bar{B}_s^0 \to K_0^{*0}\eta) = 56.2^{+1.2+0.0+7.6+17.0}_{-2.0-0.1-5.9-15.7}\,{\rm S\,II}\,,$$

$$\mathcal{A}_{CP}^{\rm dir}(\bar{B}_s^0 \to K_0^{*0}\eta') = 42.4^{+1.1+0.1+7.0+8.5}_{-3.1-0.1-5.9-10.1}\,{\rm S\,II}\,,$$

where the uncertainties are mainly from the B_s meson shape parameter $\omega_b = 0.5\pm0.05$, the decay constant $\bar{f}_{K_0^*}$, the Gegenbauer moments B_1 and B_3 of the scalar meson K_0^*, and the CKM angle $\alpha = (100\pm20)^\circ$. These values of the direct CP-violating asymmetries are sensitive to the variations of the CKM angle α, their dependences on the CKM angle α are shown in Fig. 2.

From Table 3, we find that if one neglects the contributions from the nonfactorizable annihilation diagrams, their branching ratios and the direct CP-violating asymmetries between these two decay modes tend to be near each other, respectively. When we include these contributions, the branching ratios of these two decays both become small, and the change for the decay mode $\bar{B}_s^0 \to K_0^{*0}(1430)\eta$ is larger. In Scenario I, the branching ratios for each decay are sensitive to the contributions from the factorizable annihilation diagram contributions: If we neglect them, the branching ratios increase by more than 3 times. This is because the weak annihilation amplitudes receive a larger real part for S I compared with those in S II. The direct CP-violating asymmetries also have a great dependence on the annihilation contributions, especially for the decay $\bar{B}_s^0 \to K_0^{*0}(1430)\eta'$. Neglecting either of the annihilation type contributions, the value of the direct CP-violating asymmetries will become small. In the PQCD approach, annihilation diagrams are an important source for CP asymmetries.

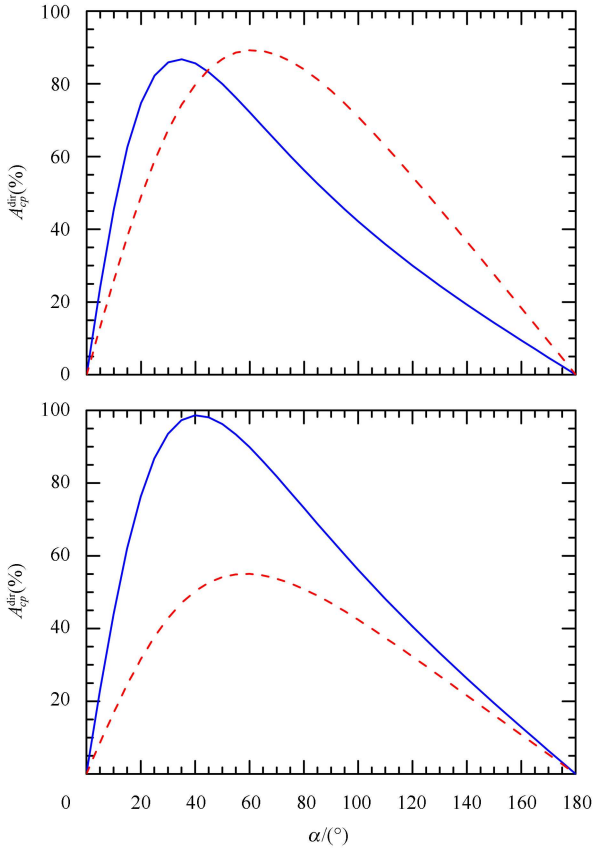

Fig. 2. The dependence of the direct CP-violating asymmetries for $\bar{B}_s^0 \to K_0^{*0}(1430)\eta$ (solid curve) and $\bar{B}_s^0 \to K_0^{*0}(1430)\eta'$ (dashed curve) on the Cabibbo-Kobayashi-Maskawa angle α. The up (down) panel is plotted in Scenario I (II).

Table 3. Branching ratios (top; in units of $\times 10^{-7}$) and direct CP-violating asymmetries (bottom; in units of %) of decays $\bar{B}_s^0 \to K_0^*(1430)\eta^{(\prime)}$. Column (1) represents the full contribution, Columns (2) and (3) are for the contributions after neglecting the nonfactorizable and the factorizable annihilation diagrams, respectively. Column (4) is for the contributions after ignoring both of these annihilation diagrams.

decay mode	(1)	(2)	(3)	(4)
$\mathcal{B}(\bar{B}_s^0 \to K_0^{*0}\eta)$(S I)	3.85	7.49	13.70	13.33
$\mathcal{B}(\bar{B}_s^0 \to K_0^{*0}\eta')$(S I)	5.17	8.04	16.05	16.70
$\mathcal{B}(\bar{B}_s^0 \to K_0^{*0}\eta)$(S II)	3.87	7.29	4.23	3.82
$\mathcal{B}(\bar{B}_s^0 \to K_0^{*0}\eta')$(S II)	7.75	8.08	4.77	5.27
$\mathcal{A}_{CP}^{\rm dir}(\bar{B}_s^0 \to K_0^{*0}\eta)$(S I)	42.1	40.0	32.7	31.4
$\mathcal{A}_{CP}^{\rm dir}(\bar{B}_s^0 \to K_0^{*0}\eta')$(S I)	70.9	45.0	36.7	37.3
$\mathcal{A}_{CP}^{\rm dir}(\bar{B}_s^0 \to K_0^{*0}\eta)$(S II)	56.2	45.8	34.2	39.1
$\mathcal{A}_{CP}^{\rm dir}(\bar{B}_s^0 \to K_0^{*0}\eta')$(S II)	42.4	39.5	−11.6	−12.4

5 Conclusion

In this paper, we calculate the branching ratios and the CP-violating asymmetries of decays $\bar{B}_s^0 \to K_0^{*0}(1430)\eta^{(\prime)}$ in the PQCD factorization approach and find the following results:

1) The branching ratios of the decay of $\bar{B}_s^0 \to K_0^{*0}(1430)\eta$ and $\bar{B}_s^0 \to K_0^{*0}(1430)\eta'$ are both in the order of 10^{-7}, and $\mathcal{B}(\bar{B}_s^0 \to K_0^{*0}(1430)\eta)$ is smaller than $\mathcal{B}(\bar{B}_s^0 \to K_0^{*0}(1430)\eta')$ in each scenario.

2) For the direct CP-violating asymmetries, the theoretical predictions in the PQCD approach are large and sensitive to the variation of the CKM angle α. As the lattice calculations, if one can suppose that $K_0^*(1430)$ is the lowest-lying P-wave $q\bar{q}$ scalar meson, then

$$\mathcal{A}_{CP}^{\rm dir}(\bar{B}_s^0 \to K_0^{*0}(1430)\eta) = 56.2^{+18.7}_{-16.9}, \quad (29)$$

$$\mathcal{A}_{CP}^{\rm dir}(\bar{B}_s^0 \to K_0^{*0}(1430)\eta') = 42.4^{+11.1}_{-12.1}. \quad (30)$$

3) The contributions from the annihilation diagrams are very important, they play an important role in accounting for future data. The interference with other type contributions can have a large effect on the branching ratio and the direct CP-violating asymmetry.

References

1 Tornqvist N A. Phys. Rev. Lett., 1982, **49**: 624
2 Jaffe G L. Phys. Rev. D, 1977, **15**: 267; Phys. Rev. D, 1977, **15**: 281; Kataev A L. Phys. Atom. Nucl., 2005, **68**: 567; Vijande A, Valcarce A, Fernandez F and Silvestre-Brac B. Phys. Rev. D, 2005, **72**: 034025
3 Weinstein J, Isgur N. Phys. Rev. Lett., 1982, **48**: 659; Phys. Rev. D, 1993, **27**: 588; 1990, **41**: 2236; Locher M P et al. Eur. Phys. J. C, 1998, **4**: 317
4 Baru V et al. Phys. Lett. B, 2004, **586**: 53
5 Celenza L et al. Phys. Rev. C, 2000, **61**: 035201
6 Strohmeier-Presicek M et al. Phys. Rev. D, 1999, **60**: 054010
7 Close F E, Kirk A. Phys. Lett. B, 2000, **483**: 345
8 Charng Y Y, Kurimoto T, LI Hsiang-Nan. Phys. Rev. D, 2006, **74**: 074024; Phys. Rev. D, 2008, **78**: 059901
9 XIAO Zhen-Jun, GUO Dong-Qing, CHEN Xin-Fen. Phys. Rev. D, 2007, **75**: 014018
10 Giri A K, Mawlong B, Mohanta R. Phys. Rev. D, 2006, **74**: 114001
11 CHENG Hai-Yang, YANG Kwei-Chou. Phys. Rev. D, 2005, **71**: 054020
12 CHENG Hai-Yang, CHUA Chun-Khiang, YANG Kwei-Chou. Phys. Rev. D, 2006, **73**: 014017
13 CHENG Hai-Yang, CHUA Chun-Khiang, YANG Kwei-Chou. Phys. Rev. D, 2008, **77**: 014034
14 ZHANG Zhi-Qing, XIAO Zhen-Jun. Chin. Phys. C (HEP & NP), 2010, **34**(5): 528
15 ZHANG Zhi-Qing, ZHANG Jun-Deng. Eur. Phys. J. C, 2010, **67**: 163
16 ZHANG Zhi-Qing. Phys. Rev. D, 2010, **82**: 034036
17 CHENG Hai-Yang, CHUA Chun-Khiang. Phys. Rev. D, 2010, **82**: 034014
18 Grozin A G, Neubert M. Phys. Rev. D, 1977, **55**: 272; Beneke M, Feldmann T. Nucl. Phys. B, 2001 **592**: 3
19 Kawamura H et al. Phys. Lett. B, 2003, **523**: 111; Mod. Phys. Lett. A, 2003, **18**: 799
20 LÜ Cai-Dian, YANG Mao-Zhi. Eur. Phys. J. C, 2003, **28**: 515
21 XIAO Zhen-Jun, ZHANG Zhi-Qing, LIU Xin et al. Phys. Rev. D, 2008, **78**: 114001
22 LI Hsiang-Nan. Phys. Rev. D, 2002, **66**: 094010
23 LI Hsiang-Nan, Tseng B. Phys. Rev. D, 1998, **57**: 443
24 ZHANG Zhi-Qing. Eur. Phys. J. C, 2010, **69**: 433
25 ZHANG Zhi-Qing. J. Phys. G, 2010, **37**: 085012
26 Buchalla G, Buras A J, Lautenbacher M E. Rev. Mod. Phys., 1996, **68**: 1125
27 http://www.slac.stanford.edu/xorg/hfag
28 Ali A et al. Phys. Rev. D, 2007, **76**: 074018
29 Aubert B et al. (BABAR collaboration). Phys. Rev. D, 2008, **78**: 011107
30 Mathur N et al. Phys. Rev. D, 2007, **76**: 114505
31 Beneke M, Neubert M. Nucl. Phys. B, 2003, **675**: 333
32 WANG Hui-Sheng, LIU Xin, XIAO Zhen-Jun et al. Nucl. Phys. B, 2006, **738**: 243